



Article

# Study on the Propagation of Stress Waves in Natural Fiber Composite Strips

Antigoni K. Barouni <sup>1,\*</sup> and Christoforos S. Rekatsinas <sup>2</sup>

<sup>1</sup> School of Mechanical and Design Engineering, University of Portsmouth, Portsmouth PO3 1DJ, UK

<sup>2</sup> School of Mechanical Aeronautics Engineering, University of Patras, 26500 Patras, Greece; xrek@upatras.gr

\* Correspondence: antigoni.barouni@port.ac.uk

**Abstract:** The propagation of Lamb waves within the structure of natural fiber reinforced composite strips is investigated using a semi-analytical solution and a time domain spectral finite element numerical method. The need to monitor the structural health of natural fiber reinforced composites is becoming greater, as these sustainable composites are being increasingly used in various industrial applications in automotive and marine structures. Three different types of flax fiber composites were studied and the fundamental wave modes were excited on the structure. Both methods under consideration were able to capture the symmetric and antisymmetric wave modes for all the material configurations. Especially the complex nature of a hybrid flax/glass fiber composite was studied and results were very promising for future damage investigation. Further to this, an attempt was made to excite the hybrid strip at higher frequency and the study revealed the potential to capture all the existing wave modes.

**Keywords:** natural fiber composites; flax fibers; Lamb wave propagation; semi-analytical; time domain spectral elements; structural health monitoring



**Citation:** Barouni, A.K.; Rekatsinas, C.S. Study on the Propagation of Stress Waves in Natural Fiber Composite Strips. *J. Compos. Sci.* **2021**, *5*, 34. <https://doi.org/10.3390/jcs5010034>

Received: 9 November 2020

Accepted: 15 January 2021

Published: 19 January 2021

**Publisher's Note:** MDPI stays neutral with regard to jurisdictional claims in published maps and institutional affiliations.



**Copyright:** © 2021 by the authors. Licensee MDPI, Basel, Switzerland. This article is an open access article distributed under the terms and conditions of the Creative Commons Attribution (CC BY) license (<https://creativecommons.org/licenses/by/4.0/>).

## 1. Introduction

Natural fiber-reinforced plastics have gained increasing interest among various industrial applications, such as automotive, maritime structures, buildings and infrastructure as well as food containers. The increasing negative effect on the environment and climate change as a result of the increasing use of fossil-based materials has driven the interest worldwide from nonrenewable fossil-based composite reinforcements (such as glass and carbon fibers) to more sustainable and environmentally friendly materials, such as plant fiber-based reinforcements [1–3]. Their very good mechanical properties, combined with their lightweight structure and their environmentally friendly nature and recyclable properties have made them replace conventional composites often in secondary structures and, in some cases, in load-bearing primary structures. The main advantage of natural fibers lies in their environmental attributes; being biodegradable, recyclable and renewable makes them attractive for various applications, considering also the mitigation of energy required to be consumed for their production and processing compared to carbon and glass fibers [4,5].

The need to investigate the health status of structures via different nondestructive testing (NDT) methods and decide on their structural health condition is crucial in any application. Structural health monitoring (SHM) of composite structures using wave propagation methods has been used extensively the last decades in order to identify, locate and measure the size and depth of defects and cracks in those structures [6]. Analyzing the wave characteristics of structures and the propagation of elastic waves through media and components has been attempted from many researchers and has been implemented in real applications. Numerical and experimental methods are compared and validated in order to provide a robust strategy in the damage identification problem within a structure [7]. The findings from the investigation of the damage state in composite structures using wave propagation methods become hard to interpret because of the complex nature of the

material, its heterogeneity and layered structure. In these structures, their geometry and anisotropic material behavior are complicated, any analytical solutions become difficult and sometimes impossible to formulate and, hence, solve. Therefore, semi-analytical and numerical methods have been developed for the computation of dispersion curves and the simulation of the propagation of stress waves within these structures. Solutions for 2D strips and 3D plates provide a very good understanding of the ultrasonic waves that propagate and their characteristics [8–10]. The application of finite spectral elements has been also used to simulate and understand the one-dimensional propagation of elastic waves in rods and beams where their efficiency has been proved over the classic finite element approach [11]. Other solutions involve the use of piezoelectric actuators and sensors for the excitation of the structures and detection of its behavior [8,12].

The use of wave propagation methods in conventional composites is extensively used in a wide range of applications and structures. However, the use of these methods on sustainable, natural fiber composites is very limited and only a few works have been focused on this direction. Studies where various structural health monitoring methods have been applied to both conventional and natural fiber composites and comparing their capabilities have provided interesting outputs. Most of the SHM methods can be equally applied to both material systems with relative sensitivity. The use of visual inspection methods and piezoelectric actuators was implemented in wind turbine blades made out of glass fiber composite and flax fiber composite when a lightning strike was experimentally simulated, and the results were compared [13]. The comparison revealed that the SHM methods were applicable to both material systems and concluded that the flax reinforced-composite could be a good replacement of glass fibers. Generally, the effective application of an SHM technique strongly depends on the deep understanding of the mechanical properties of the material [14]. Especially with the hybridization of the natural fiber composites with synthetic fibers to enhance their performance, the understanding of the damage mechanisms has become even more challenging in terms of interpreting the outcomes of SHM methods. An interesting approach was attempted by Muda and Mustafa [15], where a kenaf composite patch was attached to a carbon fiber aircraft panel and its performance was monitored and detected under mechanical testing using piezoelectric patches. The resemblance of the signals detected from both the undamaged and the patched specimens indicates that the SHM method used can be sensitive for natural fibers as well and that kenaf reinforced patches are a promising alternative in repair applications. The experimental extraction of dispersion curves for flax fiber composite panels have been attempted having good agreement with numerical results [16], where both the finite element (FE) and the wave finite element (WFE) methods were used and compared. Other ultrasonic testing methods have been used in order to investigate the effect of the parameters of the composite on the sound speed of the propagating wave [17]. In this case, the characteristics of the propagating waves and their changes due to the fiber content or humidity within the structure determine the state of the structure and become a tool for its evaluation. It is a fact that water and moisture absorption tendency of the flax fibers is a factor that reduces their composites' rigidity and needs to be well understood [18]. This process was extended to the full characterization of fiber content and distribution of flax reinforced composites in [19], where empirical models were proposed to correlate fiber content with longitudinal sound speed and attenuation coefficient. Recent studies have been conducted on experimental investigation of acoustic and vibration characteristics of flax fiber-reinforced composites, by studying the changes in natural frequencies and damping characteristics of the structures under various loading conditions [20]. The study concludes that this material could be used as a noise mitigation solution in aircraft and marine industry with low and medium frequency range. In another study, the vibroacoustic behavior of biodegradable composites with natural fibers was studied, where the type of the plasticizer used in the composite changes the suppression parameter of vibroacoustic behavior [21]. The thermomechanical properties of natural fiber polymer composites are very important, especially around the interface between the matrix and the reinforcement. Very recent studies [22] evaluate the

influence of thermal stresses on the fiber–matrix interface using jute fibers as reinforcement and the results were verified with nonlinear acoustic techniques. However, the ultimate aim of these studies is to evaluate, identify and locate the damages within the structures. Acoustic emission is one of the most widely used methods for this purpose and it has been used for flax-reinforced composites to study the sensitivity of sound waves to crack propagation [23]. The importance of assessing wave characteristics of newly developed and promising materials, such as natural fiber composites, has motivated this study, given the growing interest of the automotive and energy sector on these materials. The increasing interest in the design of new sustainable materials and their implementation in various structural components has driven the authors to investigate and understand how stress waves would travel in these materials and the potential of using wave propagation methods as a damage identification and localization method in these materials.

Although pure analytical approaches offer fast and accurate results, their formulation for laminated composite plates is complicated and cumbersome, hence they are effectively limited to rather simple geometries and material configurations. On the other hand, common numerical methods, such as finite element and finite difference methods, require very high spatial discretizations over the plane of the plate and through the thickness to yield converging solutions in terms of wave dispersion data and group velocities. Particularly, at high ultrasonic frequencies, where more complex wave modes are excited, the application of numerical methods becomes a computationally intractable task, involving an extremely high number of elements. This has driven research towards more efficient semi-analytical methods for the prediction of guided waves in laminated composite plates improving the robustness, accuracy and computational speed for the solution extraction. The incorporation of 2D or 3D layerwise laminate plate theories in semi-analytical solutions has increased their popularity and accuracy in wave propagation problems. Similarly, the application of explicit time domain spectral finite element (TDSFE) method combines several advantages over the classic finite element methods, especially because of the layerwise configuration through the thickness of the laminate, making it ideal for capturing of the propagation of Lamb waves.

In this paper, the propagation of stress waves in flax fiber reinforced composite strips is being investigated and verified using two different methods. A semi-analytical method, that utilizes the layerwise theory for the through-the-thickness displacement field and an analytical expression of the displacement along the length of the strip, is compared to a time domain spectral finite element (TDSFE) method, where third order Hermite polynomial splines are employed for the approximation of displacements through the thickness. Three different material configurations are used, namely a unidirectional flax-PE (PE: Polyethylene) composite strip, a woven flax fiber-reinforced composite strip and a hybrid flax/glass fiber reinforced-vinylester composite strip. The first case was verified with already existing literature. For the last two cases, both methods provided an excellent agreement for the time response. Further to this, through-the-thickness displacement field variations as well as stress and strains were presented, and the complex nature of the composites was captured.

## 2. Theoretical Background

For the formulation of the problem, the layerwise theory was used for the kinematic assumptions through the thickness of the composite strip, whereas an analytical approach of displacement was implemented along the length of the strip [9,10].

Considering the stress equilibrium equations for a plane strain problem (as depicted in Figure 1b):

$$\begin{aligned}\sigma_{x,x}(x,z,t) + \sigma_{xz,z}(x,z,t) &= \rho \ddot{u}(x,z,t) \\ \sigma_{xz,x}(x,z,t) + \sigma_{z,z}(x,z,t) &= \rho \ddot{w}(x,z,t)\end{aligned}\quad (1)$$

where  $\sigma_x$ ,  $\sigma_z$ ,  $\sigma_{xz}$  are the normal and shear stresses;  $u$ ,  $w$  are the displacement components along  $x$  and  $z$  axes, respectively;  $\rho$  is the density of the medium; the “comma” subscript

denotes differentiation with respect to  $x$  or  $z$ ; whereas double dots denote differentiation with respect to time.

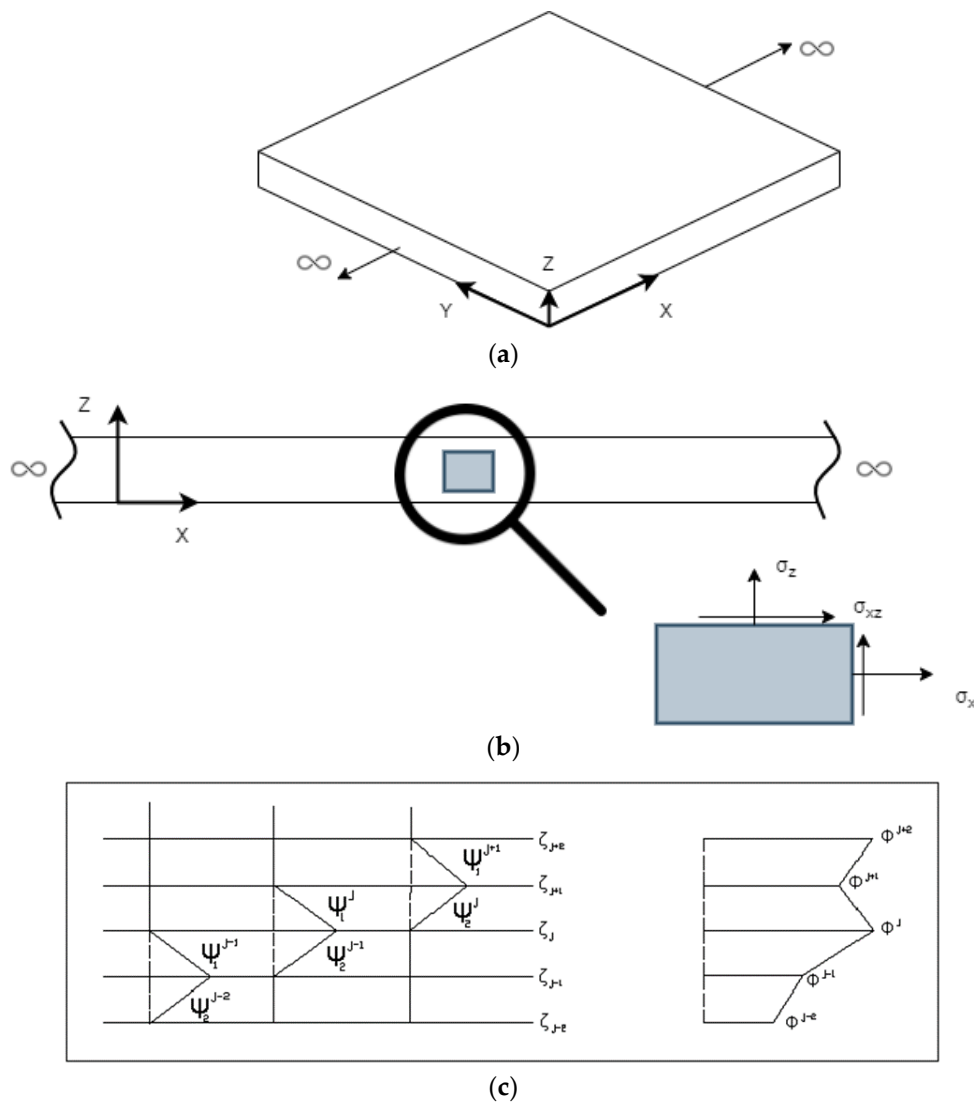


**Figure 1.** (a) 3D body with  $xyz$  coordinate system; (b) 2D case of an infinite strip  $xz$  plane with the stresses developed on an element; (c) through-the-thickness displacement field using layerwise theory.

The kinematic assumptions for the displacement field through the thickness of the laminate, as derived using the layerwise theory are given by:

$$\begin{aligned}
 u(x, z, t) &\cong \sum_{n=1}^N U^n(x, t) \Psi^n(z) \\
 w(x, z, t) &\cong \sum_{n=1}^N W^n(x, t) \Psi^n(z)
 \end{aligned}
 \tag{2}$$

where superscripts  $n = 1, \dots, N$  indicate the discrete layer,  $U^n, W^n$  are the in-plane displacements at the interfaces of each discrete layer along the  $x$  and  $z$  axes, respectively, and  $\Psi^n(z)$  are linear interpolation functions through the laminate thickness for the  $n$ th layer, as shown in Figure 1c. Substituting Equation (2) into the equilibrium Equation (1),

using strain-displacement relations and applying an analytic Fourier transform both in the time and space domain, the final problem becomes:

$$\left( \begin{bmatrix} \zeta^2 A_{11}^{mn} + D_{55}^{mn} & -i\zeta(B_{13}^{mn} - \bar{B}_{55}^{mn}) \\ -i\zeta(B_{55}^{mn} - \bar{B}_{13}^{mn}) & \zeta^2 A_{55}^{mn} + D_{33}^{mn} \end{bmatrix} - \omega^2 \begin{bmatrix} m^{mn} & 0 \\ 0 & m^{mn} \end{bmatrix} \right) \begin{Bmatrix} \hat{U}^n \\ \hat{W}^n \end{Bmatrix} = \begin{Bmatrix} \hat{F}_{xz} \\ \hat{F}_z \end{Bmatrix} \quad (3)$$

where the matrices  $A_{ij}$ ,  $B_{ij}$ ,  $D_{ij}$  represent the generalized in-plane and out-of-plane system matrices,  $m_{ij}$  are the generalized laminate mass matrices,  $\hat{F}_{xz}$  and  $\hat{F}_z$  are the shear and normal external forces, respectively,  $\omega$  is the frequency and  $\zeta$  is the wavenumber, as extracted by the Fourier transforms. The solution of the homogeneous system of Equation (3) yields the dispersion relation for elastic guided waves in 2D strips.

Using the necessary transformations, Equation (3) can be solved for a specific excitation frequency and yield the corresponding wavenumbers. Then, the inverse Fourier transform is used twice to return the time-space domain and receive the solution of the problem.

The multi-field cubic spline layerwise theory is formulated for composite and sandwich laminates to capture straight-crested symmetric and antisymmetric stress waves. Third order Hermitian polynomials are employed in the approximation of displacements through the thickness. The multinode TDSFE formulation entails displacement degrees of freedom at nodes collocated with Gauss–Lobatto–Legendre integration points facilitating the formulation of semidiagonal mass matrices. The third order through-the-thickness approximation, as well as the high order Lagrangian  $C_0$  polynomial shape functions minimize the discretization effort through the thickness to one layer per material and to 5.5 nodes per wavelength along the strip’s length in order to attain a converged and accurate solution [8].

### 3. Materials and Fabrication

In this work, the dispersion characteristics of a flax fiber-reinforced composite material are extracted and compared with experimental results from already existing literature [16]. A unidirectional flax fiber-reinforced composite laminate was used with polyethylene (LLPDE) film used as matrix material and total laminate thickness of 3.6 mm.

Then, a flax/vinyl ester woven laminate and a hybrid flax-glass fiber reinforced vinyl ester composite material are investigated and Lamb wave propagation is examined. The matrix material used was vinyl ester resin (Scott Bader Crystic VE676-03) and at 1.5% catalyst weight was used to cure. The reinforcement was woven flax with fiber orientation  $[\pm 45]_{3s}$  biaxial stitched noncrimp fabrics of 600 g/m<sup>2</sup> in aerial weight, supplied by Net Composites Ltd. Fiber volume fraction (FVF) was 49% and void content was about 4%.

Two types of composite laminates were used in this study: a flax fiber-reinforced vinyl ester (FVE) and a flax fiber-hybridised glass fiber hybrid (FGVE) composite laminate. These materials have been used previously in another study for different experimental testing [24]. Images of the in-plane and cross-section of the laminates are depicted in Figure 2a,b, respectively. The fabric configuration was 6 layers of  $+/-45^\circ$  fabrics of glass and flax, with laminate thickness equal to 4.2 mm. The hybrid specimens were manufactured using 7 layers of G/F/G/F/G/F/G configuration, where G stands for glass and F for flax, with 4.2 mm laminate thickness (Figure 2c).

The mechanical properties of the material are given in Table 1.

**Table 1.** Mechanical properties of flax fiber reinforced composite materials.

Material	Density (kg/m <sup>3</sup> )	E <sub>11</sub> (GPa)	E <sub>22</sub> (GPa)	G <sub>12</sub> (GPa)	$\nu_{12}$
Flax-PE UD	1025	9.5	1.3	0.55	0.4
Flax-vinylester	1260	134	27.2	4.4	0.1
Glass-vinylester layer	2000	45	13	4.4	0.29

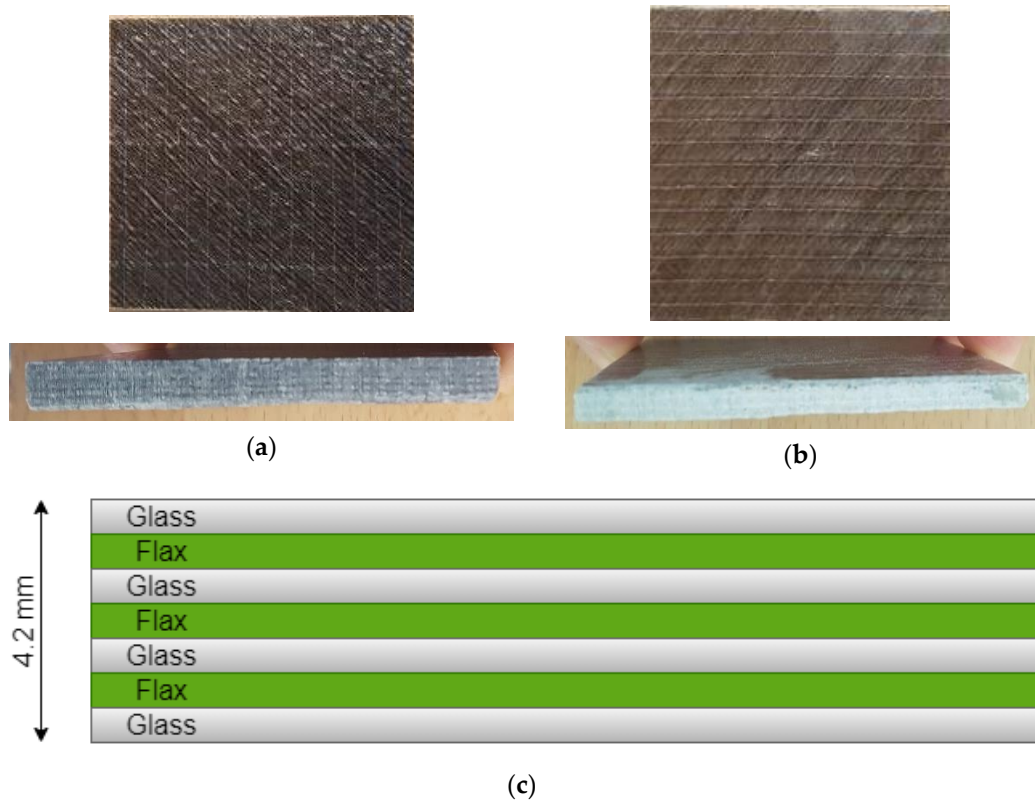


**Figure 2.** (a) Flax fiber-reinforced vinyl ester composite material; (b) flax/glass fiber-reinforced vinyl ester composite material; (c) laminate configuration for hybrid flax/glass vinylester composite strip.

#### 4. Results and Discussion

##### 4.1. Dispersion Curves Validation

The semi-analytical solution was validated with the results from [16] for the unidirectional (UD) flax-PE composite strip, by extracting the dispersion curves of the material. In Figure 3, the dispersion curves are shown, where the fundamental wave modes  $A_0$  and  $S_0$  exist solely until the frequency of 100 kHz. The dispersion curves are compared against the experimental results from [16], as shown in Figure 4, where a very good agreement was presented between the experimental results and the semi-analytical solution at the propagation direction of  $0^\circ$  and  $90^\circ$ .

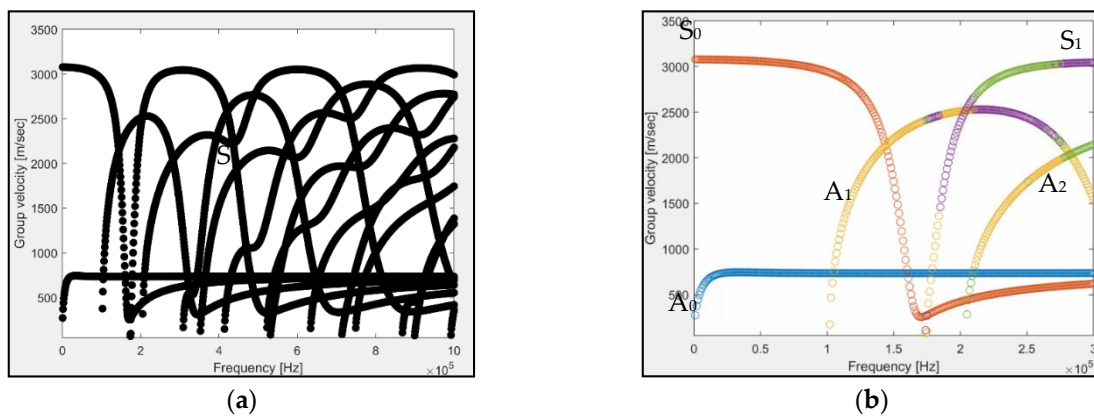


**Figure 3.** (a) Dispersion curves of flax-Polyethylene (PE) unidirectional (UD) laminate; (b) zoomed view for the first 5 Lamb wave modes.

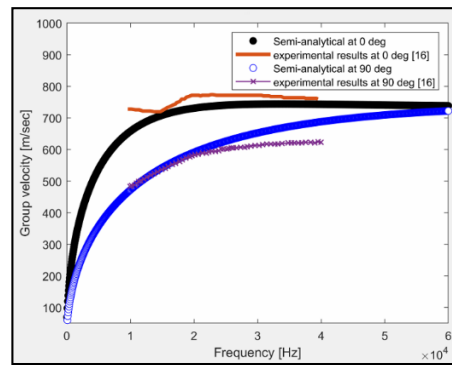


**Figure 4.** Group velocity vs. frequency for the  $A_0$  wave mode for the UD flax-PE composite strip at  $0^\circ$  and  $90^\circ$  propagation direction: validation with experimental data from [16].

Following the dispersion curves extraction described above, the time response of the strip at various points on its top surface were evaluated and presented here. The strip is being excited by a horizontal force at 45 kHz with a 4.5-cycle Hanning windowed sine pulse, as shown in Figure 5. The response was measured at 0.2 m, 0.35 m and 0.5 m from the excitation point.

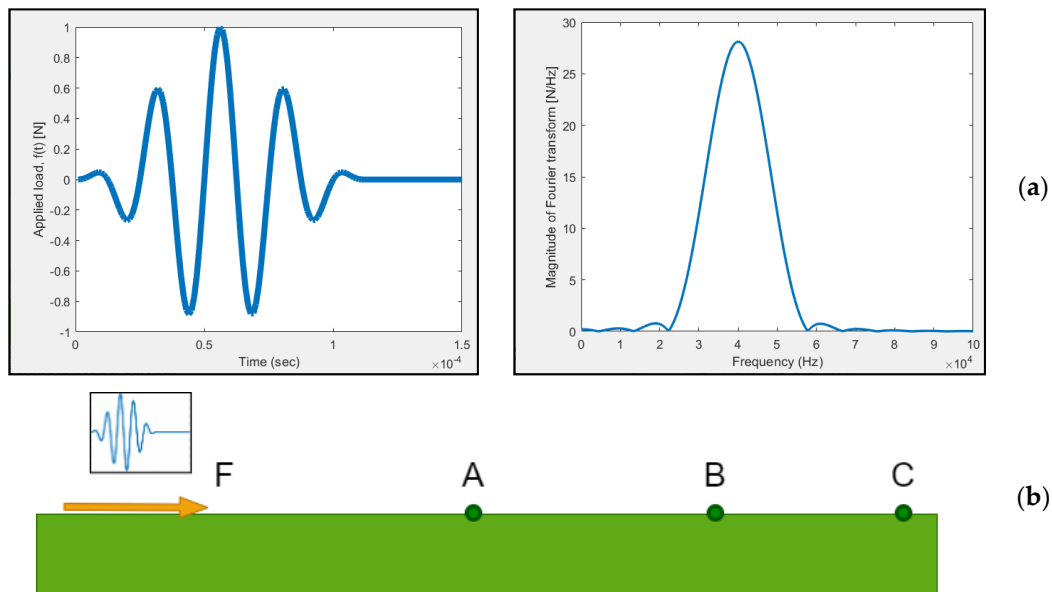


**Figure 5.** (a) 4.5 sine cycle Hanning windowed excitation pulse at 40 kHz; (b) loading case for the UD flax strip with a horizontal force  $F$ . The response of the strip was measured at the points A, B and C at 0.2 m, 0.35 m and 0.5 m, respectively, from the application point of  $F$ .

In the plots shown in Figure 6 below, the time responses of the strip using the semi-analytical solution are presented measured at points A, B and C. The responses are compared with the results from the time domain spectral finite element (TDSFE) method [8] at the same points, with an excellent agreement. In these plots, both the antisymmetric ( $A_0$ ) and the symmetric ( $S_0$ ) modes were present and they were propagating along the length of the strip, following group velocity, as given in the dispersion curves. It is also observed that the  $S_0$  was more dominant for the  $u$  displacement, whereas  $A_0$  dominated the vertical,  $w$ , displacements.

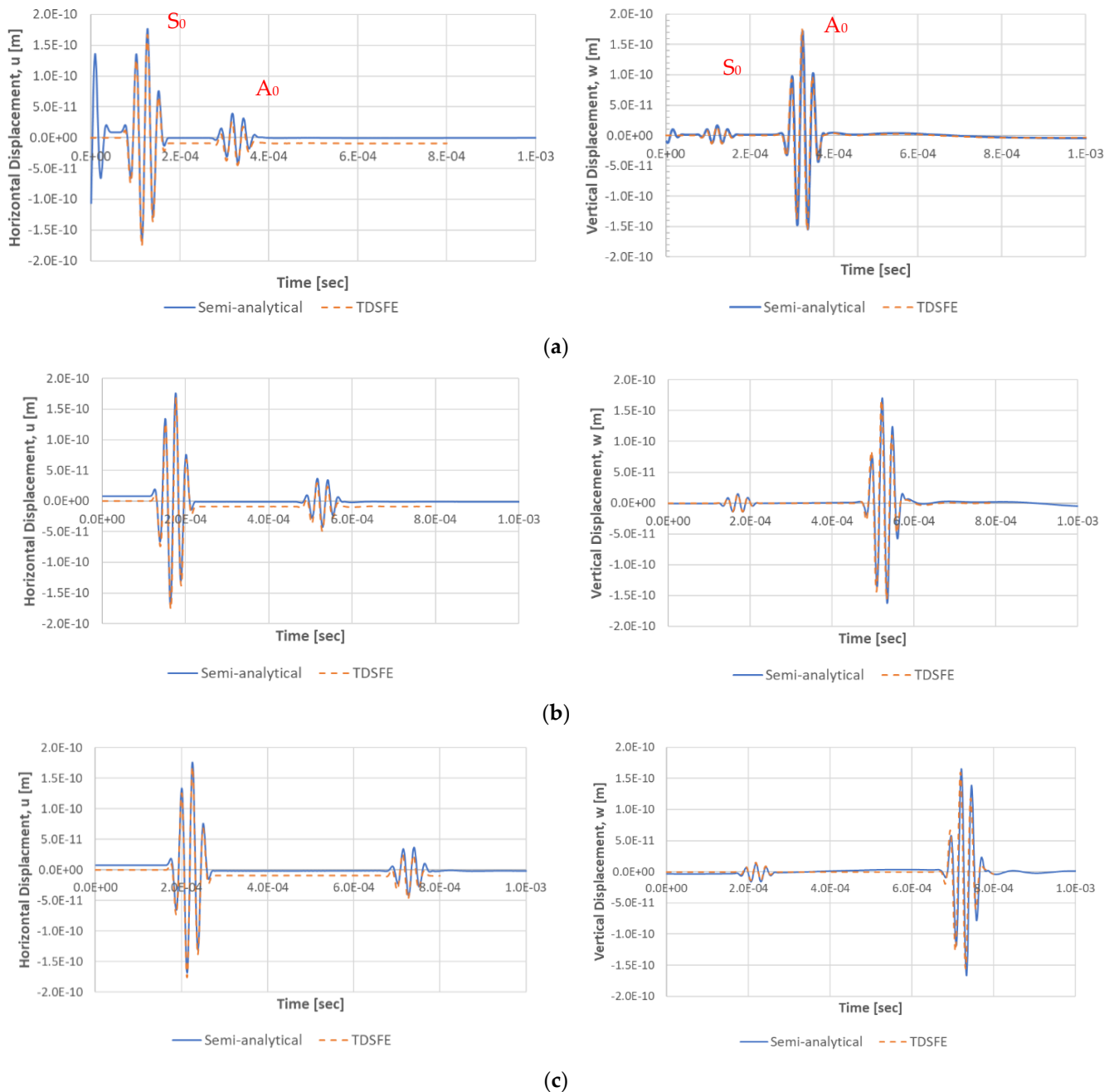


**Figure 6.** Time response of the UD flax-PE strip at various points.  $u$  displacement (left) and  $w$  displacement (right) at (a) 0.2 m, (b) 0.35 m and (c) 0.5 m from the excitation point.

#### 4.2. Flax-Vinylester Composite Strip

For the woven flax-vinylester composite strip, the dispersion curves are presented in Figure 7. The strip was excited at 50 kHz with a Hanning window of 5 sinusoidal cycles (Figure 8a). As derived from the dispersion curves in Figure 4, at 50 kHz only the wave modes  $A_0$  and  $S_0$  exist. Each mode was being excited separately, so the wave mode could be distinguished clearly. For exciting the antisymmetric mode,  $A_0$ , two vertical and opposite forces were applied on the top and bottom surfaces of the strip (Figure 8b), whereas for exciting the symmetric mode,  $S_0$ , two vertical and unidirectional vertical forces were applied on the top and bottom surfaces of the strip (Figure 8c). The support configuration of the strips for both loading conditions was free-free support, in order to



eliminate any reflections of the waves from the supports. The displacements of the top surface of the strip were evaluated at the distance of 0.35 m from the excitation point.

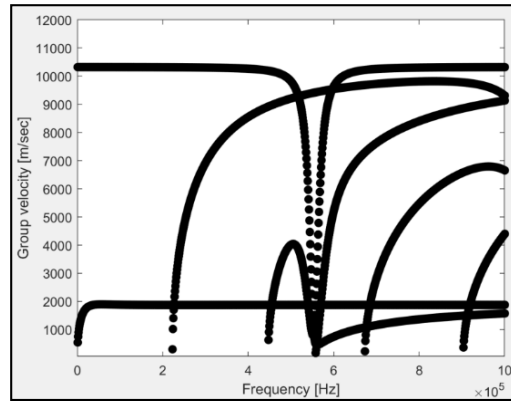


Figure 7. Group velocity vs. frequency for the woven flax fiber reinforced vinyl-ester composite strip.

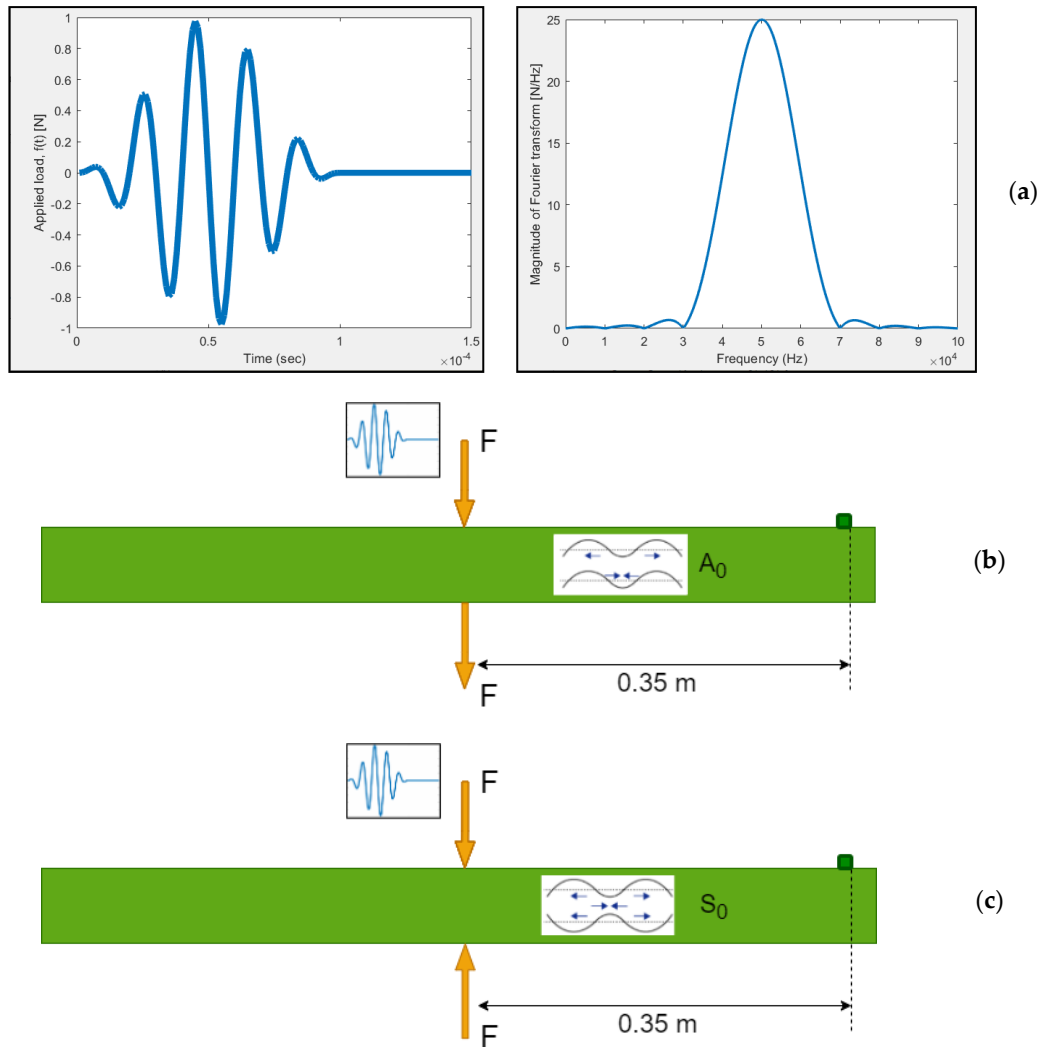
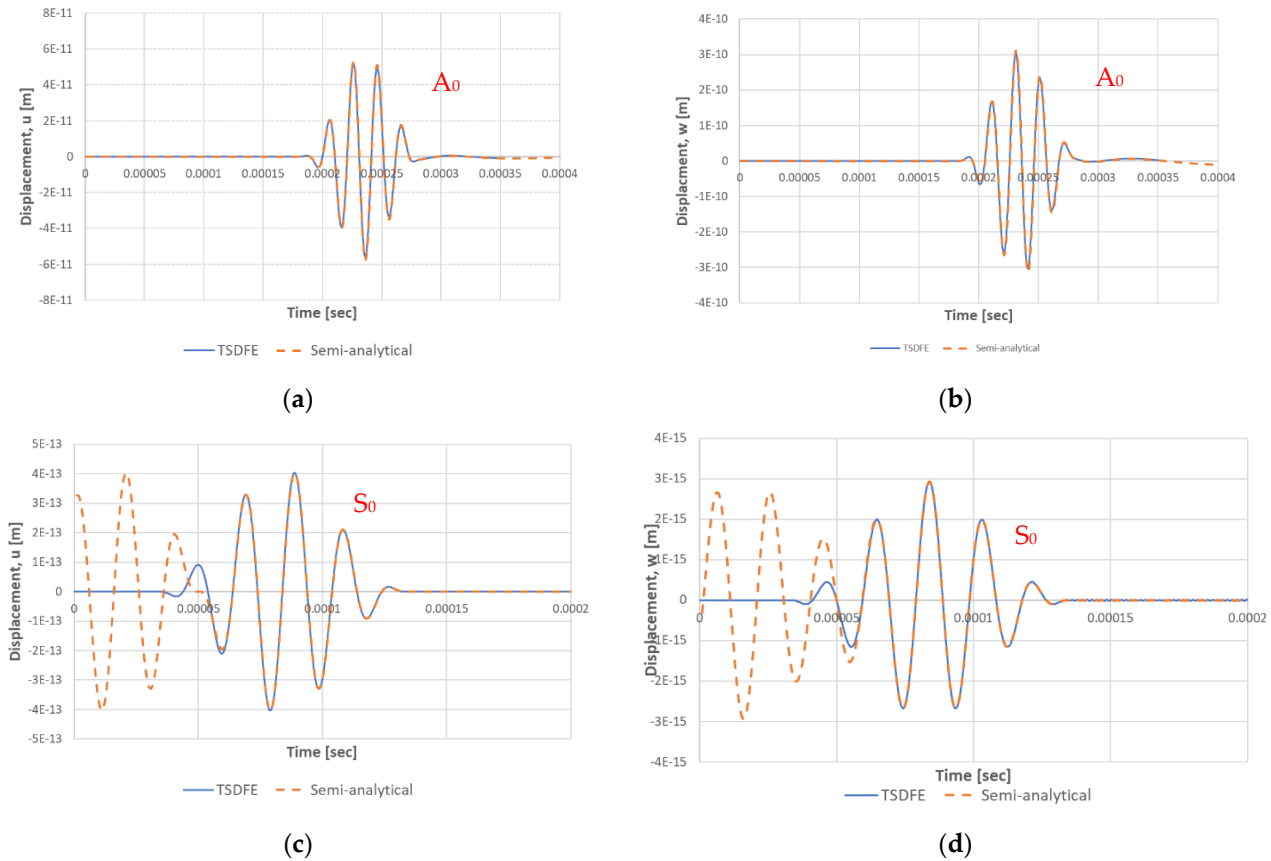


Figure 8. Loading cases for the strip under free-free support configuration. (a) 5 sine cycle Hanning windowed excitation pulse at 50 kHz; (b) excitation case of antisymmetric  $A_0$  wave mode only with vertical and opposite forces; (c) excitation case of symmetric  $S_0$  wave mode only with vertical and unidirectional forces.

The solution from the semi-analytical formulation is compared with the time domain spectral finite element (TDSFE) method for the wave propagation of composite laminates and presented in Figure 9 for each of the excitation strategies described above. As depicted in Figure 9, both solutions provided an excellent agreement, verifying the credibility of the approach to simulate the propagation of the fundamental modes in natural fiber composites, given their complex internal structure. The wave that appeared in the beginning of the response for the semi-analytical solution was derived from the inverse Fourier process and must be ignored, as it represents the excitation force.



**Figure 9.** Time response of the woven flax-vinylester composite strip at distance  $x = 0.35$  m from the excitation point, (a)  $u$  displacement when only the  $A_0$  wave mode is excited; (b)  $w$  displacement when only the  $A_0$  wave mode is excited; (c)  $u$  displacement when only the  $S_0$  wave mode is excited; (d)  $w$  displacement when only the  $S_0$  wave mode is excited.

#### 4.3. Hybrid Flax-Glass Vinylester Composite Strip

The hybrid composite strip was considered to consist of 7 layers of G/F/G/F/G/F/G configuration (Figure 2c). Using the layerwise theory, the semi-analytical model uses the appropriate kinematic assumptions to represent the continuity of the displacements between the different layers of the laminate, despite the fact that they are made of different materials.

The time response of the top surface of the strip at distance 0.35 m from the excitation point is presented in Figure 10 below for both the semi-analytical solution and the TDSFE model, based on the excitation cases, as described in the previous paragraph (Figure 8). Both solutions provided excellent agreement and complied with the wave velocities from the dispersion curves. Also, both fundamental wave modes could be identified and captured, even for this complex laminate.

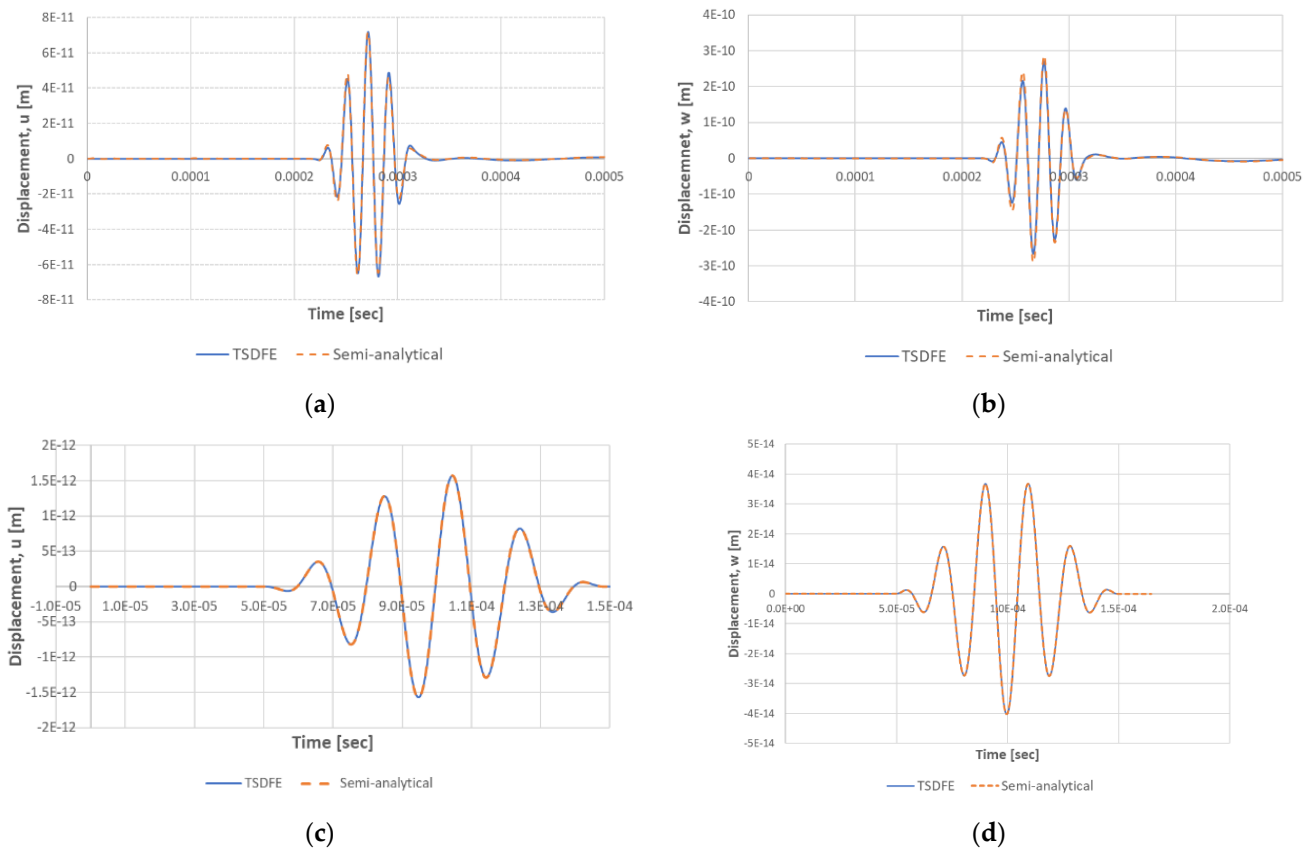


**Figure 10.** Time response of the top surface of the strip at 0.35 m from the excitation point. (a) antisymmetric  $A_0$  mode for horizontal ( $u$ ) displacements; (b) antisymmetric  $A_0$  mode for vertical ( $w$ ) displacements; (c) symmetric  $S_0$  mode for horizontal ( $u$ ) displacements; (d) symmetric  $S_0$  mode for vertical ( $w$ ) displacements.

Through-the-thickness displacements, normal and shear strains for this composite strip when excited at 50 kHz are presented in the Figure 11 below, providing further information on the displacement and strain field of the strip. The strip was excited at a point on its top surface with a vertical point load at 50 kHz. The exact location of this load did not make any difference for the semi-analytical model. However, the point load has been placed on the left-hand side end of the strip when the TSDFE was used. The data were extracted using the TSDFE method and two different data sets were considered: (a) extraction of  $A_0$  wave mode via the vertical point load and measurement of the displacement of the strip at the distance of 0.72 m away from the excitation point and at 0.5  $\mu$ sec after the load was applied (left column of the results in Figure 11) and (b) extraction of the  $S_0$  wave mode via the vertical point load and measurement of the displacements of the strip at the distance of 0.705 m away from the excitation point and at 0.15  $\mu$ sec after the load was applied (as shown in the right column of the results in Figure 11). For each measurement point the  $u$  displacement (Figure 11a,b) and  $w$  displacement (Figure 11c,d) were calculated. As it was expected, the  $u$  displacements were dominant when the  $A_0$  mode was considered, whereas the  $w$  displacements were demonstrating very small variation through the thickness. The opposite behaviour was demonstrated when the  $S_0$  mode was considered. In Figure 11e–h, the normal and shear strains for each wave mode and measurement point are presented. It is interesting to emphasise the capability of the model to capture the variant displacement and strain fields, especially in the intermediate nodes between the different materials (i.e., glass and flax layers). This capability of the model, with the higher degree terms in the theoretical background of the TSDFE method [8], makes it very promising for being able to capture any strain or stress discontinuities through the thickness of the model, which might arise from internal damage (i.e., delamination) between two adjacent layers.

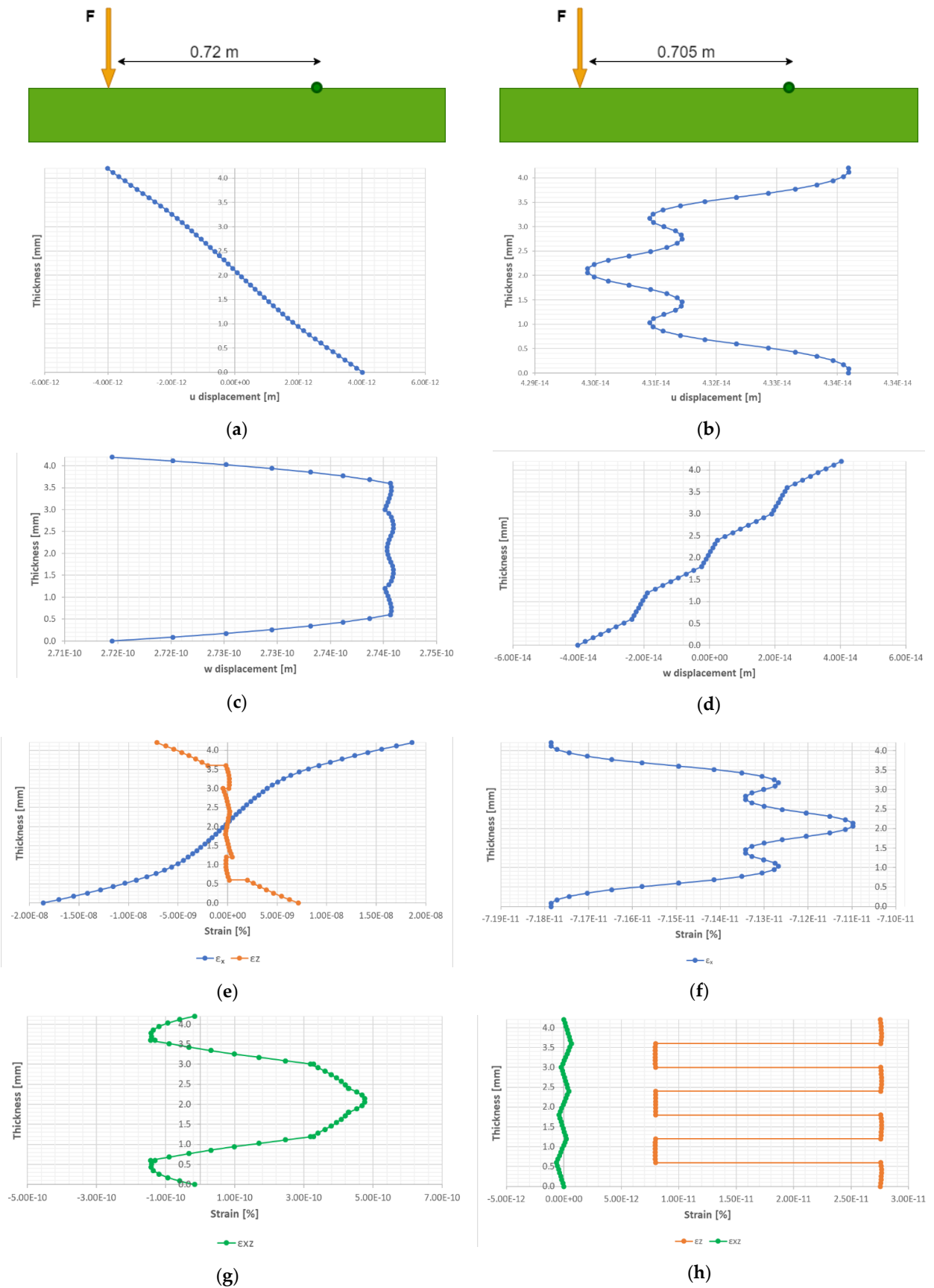


**Figure 11.** Through-the thickness-variation of the (a,b)  $u$  and (c,d)  $w$  displacements and the normal and shear strains (e–h) for the  $A_0$  (left column) and the  $S_0$  (right column) wave modes.

Further to the strains, the shear stresses were also extracted for the hybrid laminate using the TSDFE method. The interphase between the glass and flax layers nearer to the surfaces of the laminate (as circled in Figure 12a) produced a discontinuity of the shear stresses, indicating the potential of the method to capture this change.

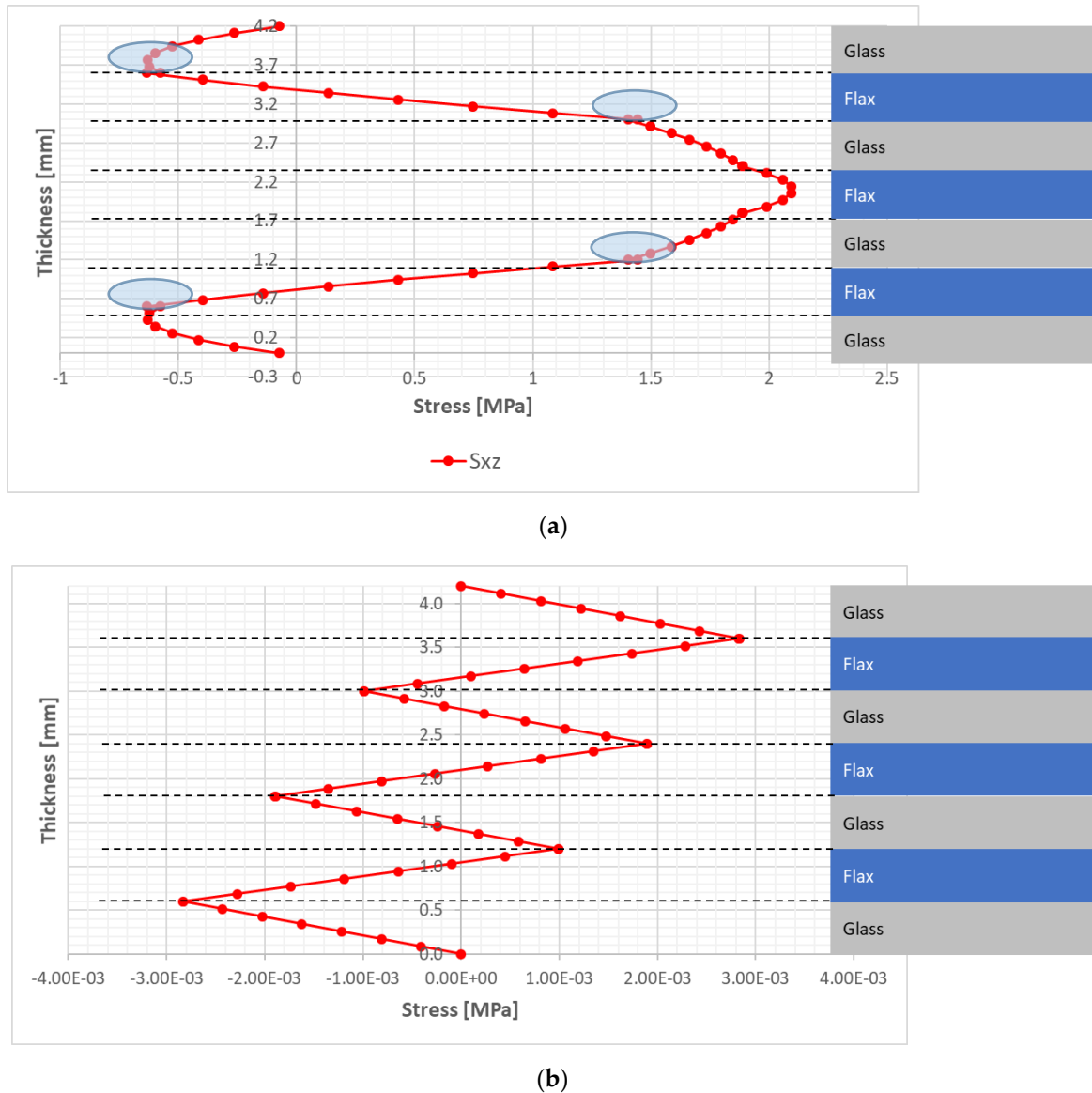


**Figure 12.** Through-the-thickness variation of the stresses for the hybrid composite laminate. (a) Shear stresses  $\sigma_{xz}$ , for  $A_0$ ; (b) shear stresses  $\sigma_{xz}$  for  $S_0$ .

The hybrid composite strip was also excited at a higher frequency in order to trigger higher wave modes. Therefore, a vertical force at 220 kHz was applied to the top surface of the strip which has been windowed again with a 5-cycle sine Hanning function. From the dispersion curves for this material (Figure 13) it can be seen that at the frequency of 220 kHz there exist three modes, i.e.,  $A_0$ ,  $S_0$  and  $A_1$ . The semi-analytical solution was used to calculate the response of the strip at this high frequency excitation. The time response of the top surface of the strip at a distance of 0.35 m from the excitation point for both the horizontal ( $u$ ) and the vertical ( $w$ ) displacement is given in Figure 14, where it clearly indicated the existence of all three present wave modes. From the time-of-flight (TOF) of each wave packet, group velocity was derived, hence it was verified that  $A_0$  travelled with 1612.9 m/s, mode  $S_0$  travelled with 6579 m/s and mode  $A_1$  travelled with 4132.2 m/s of

group velocity. Also, Figure 14a shows that  $A_1$  wave mode was very dispersive, as derived from the increased slope of the corresponding curve in the group velocity-frequency plot of Figure 13.

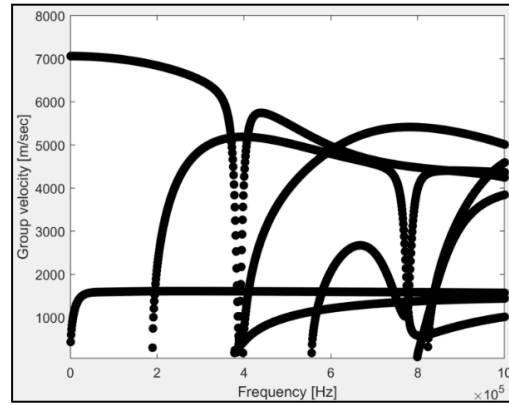
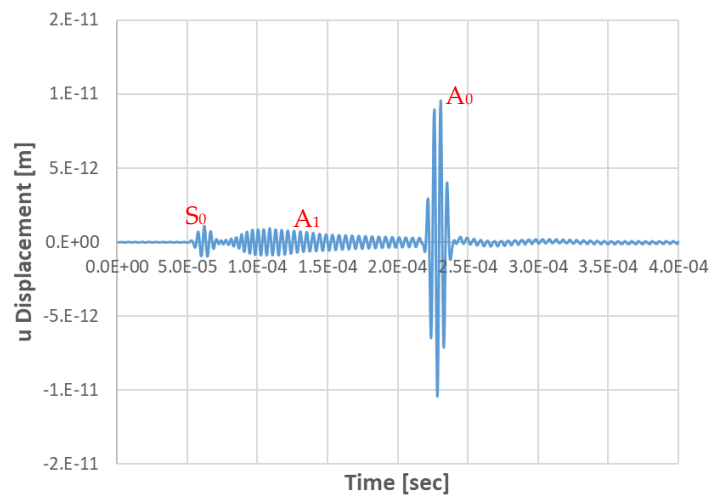
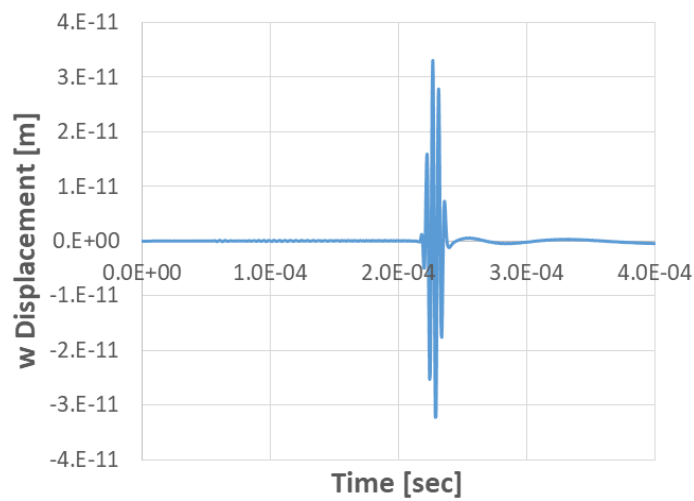


**Figure 13.** Group velocity vs. frequency for the hybrid flax-glass fiber reinforced vinyl-ester composite strip.



(a)



(b)

**Figure 14.** Time response of the top surface of the hybrid composite strip at 0.35 m away from the excitation point using the semi-analytical method. (a)  $u$  displacement; (b)  $w$  displacement.

## 5. Conclusions

In this paper, the propagation of Lamb waves was studied, and the generation of different wave modes was extracted under various loading conditions and excitations. Two different methods were used to model the propagation of elastic waves in complex laminates from natural fiber composites. The semi-analytical solution was formulated using the layerwise theory for the kinematic assumptions and solved the wave problem directly, whereas the TDSFE method modeled the structure using third order Hermite polynomial splines for the approximation of displacements through the thickness. This work demonstrated the potential of both solutions to capture stress waves that are generated along the composite strip with excellent agreement. The novel aspect of the research work relates to the ability of the proposed solutions to detect any changes of the waves as they propagate along such complex structures. As future work, these changes can be correlated to any damage or defect that can be present in the structure and, hence, identified and located.

**Author Contributions:** Conceptualization, A.K.B. and C.S.R.; data curation, A.K.B. and C.S.R.; investigation, A.K.B.; methodology, A.K.B.; writing—original draft, A.K.B.; writing—review and editing, A.K.B. and C.S.R. All authors have read and agreed to the published version of the manuscript.

**Funding:** This research received no external funding.

**Conflicts of Interest:** The authors declare no conflict of interests.

## References

1. Holbery, J. DHouston Natural-fiber-reinforced polymer composites in automotive applications. *JOM* **2006**, *58*, 80–86. [[CrossRef](#)]
2. Faruk, O.; Bledzki, A.K.; Fink, H.-P.; Sain, M. Biocomposites reinforced with natural fibers: 2000–2010. *Prog. Polym. Sci.* **2012**, *37*, 1552–1596. [[CrossRef](#)]
3. Pickering, K.L.; Efendy, M.A.; Le, T.M. A review of recent developments in natural fibre composites and their mechanical performance. *Compos. Part A Appl. Sci. Manuf.* **2016**, *83*, 98–112. [[CrossRef](#)]
4. Bourmaud, A.; Beaugrand, J.; Shah, D.U.; Placet, V.; Baley, C. Towards the design of high-performance plant fibre composites. *Prog. Mater. Sci.* **2018**, *97*, 347–408. [[CrossRef](#)]
5. Dhakal, H.N.; Zhang, Z.Y.; Richardson, M.O. Effect of water absorption on the mechanical properties of hemp fibre reinforced unsaturated polyester composites. *Compos. Sci. Technol.* **2007**, *67*, 1674–1683. [[CrossRef](#)]
6. Su, Z.; Ye, L.; Lu, Y. Guided Lamb waves for identification of damage in composite structures: A review. *J. Sound Vib.* **2006**, *295*, 753–780. [[CrossRef](#)]
7. Ostachowicz, W.; Kudela, P.; Krawczuk, M.; Zak, A. *Guided Waves in Structures for SHM*; John Wiley & Sons Ltd.: Hoboken, NJ, USA, 2012.
8. Rekatsinas, C.S.; Saravanos, D.A. A time domain spectral layerwise finite element for wave structural health monitoring in composite strips with physically modeled active piezoelectric actuators and sensors. *J. Intell. Mater. Syst. Struct.* **2016**, *28*, 488–506. [[CrossRef](#)]
9. Barouni, A.K.; Saravanos, D.A. A layerwise semi-analytical method for modeling guided wave propagation in laminated and sandwich composite strips with induced surface excitation. *Aerosp. Sci. Technol.* **2016**, *51*, 118–141. [[CrossRef](#)]
10. Barouni, A.K.; Saravanos, D.A. A layerwise semi-analytical method for modeling guided wave propagation in laminated composite infinite plates with induced surface excitation. *Wave Motion* **2017**, *68*, 56–77. [[CrossRef](#)]
11. Kudela, P.; Krawczuk, M.; Ostachowicz, W. Wave propagation in 1D structures using spectral finite elements. *J. Sound Vib.* **2007**, *300*, 88–100. [[CrossRef](#)]
12. Rekatsinas, C.S.; Saravanos, D.A. A cubic spline layerwise time domain spectral FE for guided wave simulation in laminated composite plate structures with physically modeled active piezoelectric sensors. *Int. J. Solids Struct.* **2017**, *124*, 176–191. [[CrossRef](#)]
13. Mat Daud, S.Z.; Mustapha, F.; Adzis, Z. Lightning strike evaluation on composite and biocomposite vertical-axis wind turbine blade using structural health monitoring approach. *J. Intell. Mater. Syst. Struct.* **2018**, *29*, 3444–3455. [[CrossRef](#)]
14. Jawaid, M.; Thariq, M.; Saba, N. *Structural Health Monitoring of Biocomposites, Fibre-Reinforced Composites and Hybrid Composites*; Woodhead Publishing: Cambridge, UK, 2019.
15. Muda, M.K.H.; Mustapha, F. *Composite Patch Repair Using Natural Fiber for Aerospace Applications, Sustainable Composites for Aerospace Applications*; Woodhead Publishing: Cambridge, UK, 2018.
16. Petrone, G. Dispersion curves for a natural fibre composite panel: Experimental and numerical investigation. *Aerosp. Sci. Technol.* **2018**, *82*, 304–311. [[CrossRef](#)]
17. El-Sabbagh, A.; Steuernagel, L.; Ziegmann, G. Ultrasonic testing of natural fibre polymer composites: Effect of fibre content, humidity, stress on sound speed and comparison to glass fibre polymer composites. *Polym. Bull.* **2013**, *70*, 371–390. [[CrossRef](#)]

18. Moudood, A.; Rahman, A.; Öchsner, A.; Islam, M.; Francucci, G. Flax fiber and its composites: An overview of water and moisture absorption impact on their performance. *J. Reinf. Plast. Compos.* **2018**, *38*, 323–339. [[CrossRef](#)]
19. El-Sabbagh, A.; Steuernagel, L.; Ziegmann, G. Characterization of flax polypropylene composites using ultrasonic longitudinal sound wave technique. *Compos. B Eng.* **2013**, *45*, 1164–1172. [[CrossRef](#)]
20. Huang, K.; Tran, L.Q.N.; Kureemun, U.; Teo, W.S.; Lee, H.P. Vibroacoustic behavior and noise control of flax fiber-reinforced polypropylene composites. *J. Nat. Fibers* **2019**, *16*, 729–743. [[CrossRef](#)]
21. Pawlik, A.; Frackowiak, S.; Leluk, K. The effectiveness of fiber-reinforced natural composites compared to the elastomer materials produced from nonrenewable resources in vibration transmission suppression. *Build. Acoust.* **2020**, *27*, 357–366. [[CrossRef](#)]
22. Benyamina, B.; Mokaddem, A.; Doumi, B.; Belkheir, M.; Elkeurti, M. Study and modeling of thermomechanical properties of jute and Alfa fiber-reinforced polymer matrix hybrid biocomposite materials. *Polym. Bull.* **2020**. [[CrossRef](#)]
23. Czigány, T. An acoustic emission study of flax fiber-reinforced polypropylene composites. *J. Compos. Mater.* **2004**, *38*, 769–778. [[CrossRef](#)]
24. Barouni, A.; Dhakal, H.N. Damage investigation and assessment due to low-velocity impact on flax/glass hybrid composite plates. *J. Compos. Struct.* **2019**, *226*. [[CrossRef](#)]